# Polymer Chemistry

## Accepted Manuscript

This article can be cited before page numbers have been issued, to do this please use: R. Li, X. Zhang, S. Kim, V. Mailaender, K. Landfester and C. T. J. Ferguson, *Polym. Chem.*, 2024, DOI: 10.1039/D4PY00493K.

View Article Online
DOI: 10.1039/D4PY00493K

COMMUNICATION

Received 00th January 20xx,

Accepted 00th January 20xx

DOI: 10.1039/x0xx00000x

# Therapeutic applications of responsive organic photocatalytic polymers, enabling *in situ* drug activation

*Rong Li,[a] Xueqing Zhang,[a] Seunghyeon Kim,[a] Volker Mailänder,[a] Katharina Landfester,[a]* and Calum T. J. Ferguson[b]**



**Targeted prodrug activation within the acidic tumour microenvironment is needed to limit off-target effects in chemotherapy. This in combination with photodynamic generation of reactive oxygen species (ROS) can be used for efficient remediation of cancerous tissue. To achieve this, pH-responsive polymers with photocatalytic units that become activated in the acidic pH of the tumour microenvironment have been created. Four model prodrug linkages in small molecule substrates have been investigated along with a model polymeric based prodrug. We have demonstrated the pH-dependent activation of model prodrug molecules, due to conformational changes of the pH-responsive photocatalytic polymers. Additionally, a prodrug of the common skin cancer chemotherapy drug, Fluorouracil (5FU), could be photocatalytically activated and induce cell death in cancer cells.**

The emergence of photodynamic therapy (PDT) has facilitated the minimally invasive treatment of various diseases (e.g. cancers) with well-understood fundamental mechanisms of operation. Upon light irradiation, a photocatalyst absorbs a photon generating a short-lived excited singlet state ($S_1$) that can undergo intersystem crossing and populate the more stable excited triplet state $T_1$. The energy of this excited triplet state can be further transferred to the molecular oxygen ($O_2$), generating reactive singlet oxygen $^1O_2$.[1,2] Additionally, other reactive oxygen species (ROS) such as superoxide radical $O_2^{\cdot-}$ can also be produced via an electron transfer process, which can further interact with water as solvent generating hydroxyl radicals $OH^{\cdot}$. These ROS can induce oxidative damage and ultimately kill cancer cells.[3–6] However, the performance of many currently developed photocatalyst molecules has significant limitations such as intrinsic hydrophobicity[7] and the lack of targeting towards tumour cells.[8–11] Therefore, the development of a novel tumour-specific PDT system is highly desired.

To develop a general strategy to selectively target the tumour tissue, ubiquitous features of the tumour microenvironment (for instance low pH value, high interstitial pressure, or hypoxia conditions) have been frequently selected as an alternative to endogenous biomarkers.[12] Typical systems have been designed by incorporating stimuli-responsive moieties to modulate their functionalities in response to either external (e.g. UV light[13,14]) or endogenous stimuli (e.g. enzyme,[15,16] changes in pH value ,[17–19] redox,[20] and hypoxia conditions[21,22]). Solid tumours are ubiquitously characterized by the dysregulated pH value, where the extracellular microenvironment ($pH_e$ 6.5-6.9) is slightly lower in comparison to normal tissues (pH 7.2-7.4). To this consideration, developing a pH-sensitive polymer system may achieve the targeted activation of the photocatalyst in the tumour microenvironment. Diblock polymer chains can cluster to form particles through self-assembly, where the photocatalytic segments are immobilised in the core and remain inactive in the bloodstream. If a pH-responsive group is incorporated into the polymer structure upon exposing the particle to the acidic extracellular microenvironment, photocatalytic moieties can be revealed and activated due to disassembly, during which the aqueous compatibility of the photocatalyst is also enhanced. Therefore, we propose that a pH-responsive polymer system containing photocatalytic moieties may modulate the tumour-specific production of ROS for cancer therapy.

ROS can act not only as active therapeutic agents to kill cancer cells directly but also as a trigger to control the activation of other treatment processes (e.g., prodrug activation or drug release from nanocarriers), inducing additive or even synergistic efficacies. For example, conjugating ROS-sensitive linkers[6,23] such as aminoacrylate bond,[24,25] thioketal bond,[26,27] phenylboronic ester[28–31] in the chemical structures of nanocarriers and/or drugs (generally with -OH, -NH-, or -$NH_2$ functional groups presented) have been explored for cascade reaction-driven anti-cancer drug release. Therefore, the combination of pH-responsive polymeric photocatalysts, that are capable of ROS generation, and ROS-responsive prodrug molecules could lead to the triggered drug release *in situ*, which may provide a promising strategy to enhance antitumour efficacy through PDT/chemo combination therapy.

Electronic Supplementary Information (ESI) available: [details of any supplementary information available should be included here]. See DOI: 10.1039/x0xx00000x

View Article Online
DOI: 10.1039/D4PY00493K

# COMMUNICATION

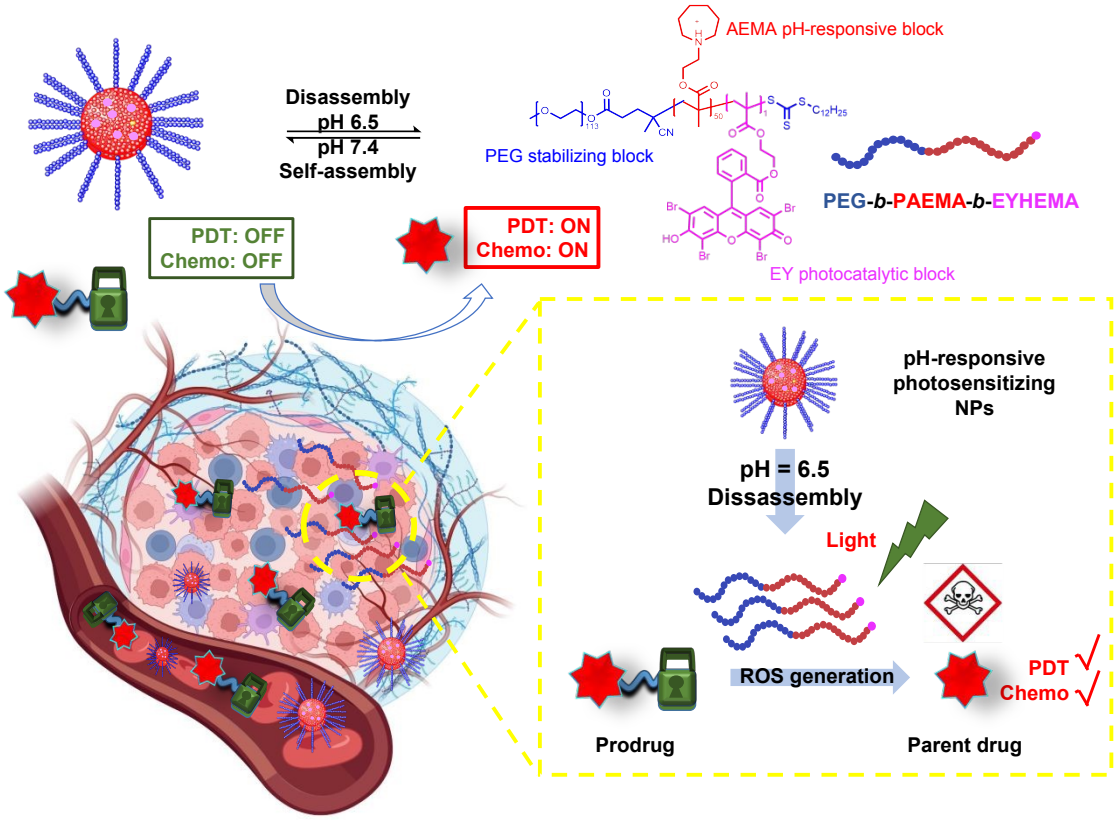


**Scheme 1.** Illustration of the pH-responsive polymer photocatalyst that can respond to subtle pH difference from normal tissue to slightly acidic tumour microenvironment, which allows the controlled activation of prodrug molecules.

Here, we have developed a pH-responsive photocatalytic system that can selectively generate ROS at tumour tissue and further activate prodrugs through a cascade reaction. To demonstrate the versatility of this photocatalytic system, the activation of four ROS-sensitive linkages, including aminoacrylate bond, thioketal bond, phenylboronic ester and oxalate, have been examined. As illustrated in Scheme 1, pH-responsive amphiphilic polymer poly(ethylene glycol)-*b*-poly(2-azepane ethylmethacrylate)-*b*-2-(methacryloyloxy)ethyl 2-(2,4,5,7-tetrabromo-3,6-dihydroxy-9H-xanthen-9-yl)benzoate $PEG_{113}$-*b*-$PAEMA_{50}$-EYHEMA was synthesized. These amphiphilic polymer chains self-assemble at pH 7.4 to form polymer particles. Once accumulated in the acidic tumour environment (pH 6.5), the hydrophobic PAEMA block of the polymer becomes protonated, leading to the disassembly of the particles and exposure of the photocatalyst eosin Y. Upon light irradiation, ROS are generated by the active eosin Y and subsequently allow the activation of prodrugs through the ROS-induced cleavage of the protecting group.

Dual-responsive copolymers $PEG_{113}$-*b*-$PAEMA_{50}$-EYHEMA were synthesized by reversible addition-fragmentation chain transfer (RAFT) polymerization using poly(ethylene glycol) methyl ether (4-cyano-4-pentanoate dodecyl trithiocarbonate) ($mPEG_{113}$-CPDTC) as the macro-chain transfer agent (macro-CTA), 2-azepane ethylmethacrylate (AEMA) and 2-(2-(2,4,5,7-tetrabromo-6-hydroxy-3-oxo-3H-xanthen-9-yl) benzamido) ethyl methacrylate (EYHEMA) as the pH-responsive and light-responsive monomers, respectively (Figure 1a). The resulting polymer was confirmed by $^1$H NMR spectroscopy and gel permeation chromatography (GPC) suggesting a number averaged molar mass of 13.9 kDa (supporting information, Figure S1 and S2). A bimodal distribution was observed, which is believed to be due to unfunctionalized PEG in the macroCTA. FTIR (Figure S3) was used to examine the chemical compositions of $PEG_{113}$-*b*-$PAEMA_{50}$ and $PEG_{113}$-*b*-$PAEMA_{50}$-EYHEMA polymer chains. The fingerprint peaks of these polymer chains, including -$CH_2$-, C=O, C-O, and C-N functional groups are clearly visible at 2750-3100 $cm^{-1}$, 1725 $cm^{-1}$, 1470 $cm^{-1}$, and 1150 $cm^{-1}$, respectively. However, the effect of the photocatalytic moiety was not observed on the FTIR

View Article Online
DOI: 10.1039/D4PY00497H

spectrum due to the low loading of the photocatalytic monomer (0.49 mol%). The optical property of the dual-responsive polymers was visualized by UV/Vis spectrum, displaying absorption in the green light region (Figure 1b) in agreement with the literature.[32]

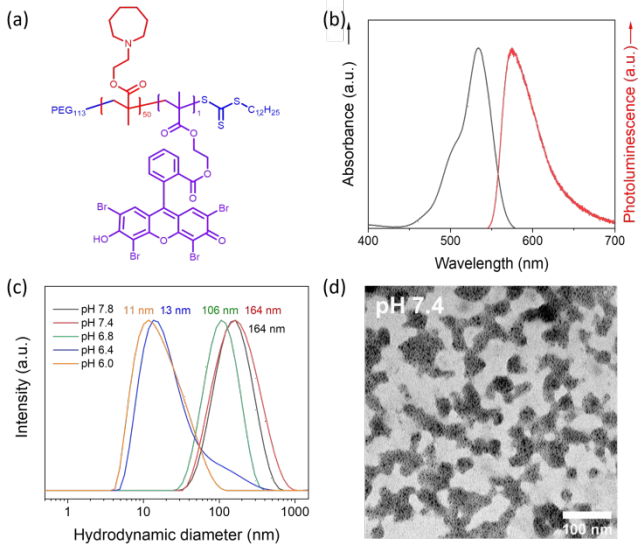


**Figure 1.** Characterizations of pH-responsive polymers. (a) Molecular structure of the designed pH-responsive photocatalytic copolymer $PEG_{113}$-*b*-$PAEMA_{50}$-EYHEMA. (b) UV/Vis absorbance and emission spectra of the $PEG_{113}$-*b*-$PAEMAH^{+}_{50}$-EYHEMA polymer chains in phosphate buffer at pH 6.5 (1 mg/mL). (c) The hydrodynamic diameter ($PEG_{113}$-*b*-$PAEMA_{50}$) changes as a function of pH value measured by DLS. (pH 6.0, 6.5, 6.8, 7.2, 7.4, and 7.8, 0.1 mM) (laser: 632.8 nm). (d) TEM image of NP-AEMA-EY nano-assembly in PBS pH 7.4.

PAEMA has been specifically developed as an ultra-pH-sensitive polymer that responds to a ~0.3 pH increment[17,19,33], aligning perfectly with the pH difference of the extracellular microenvironment ($pH_e$ 6.5-6.9) compared to normal tissues (pH 7.2-7.4).[34] Taking advantage of this ultrasensitive pH-responsiveness of PAEMA, $PEG_{113}$-*b*-$PAEMA_{50}$ can be protonated at pH 6.5, leading to the solvation of the polymer chains, while deprotonated at pH 7.4, resulting in an amphiphilic diblock copolymer and self-assembly. Therefore, pH-sensitive nano-assemblies were prepared by self-assembly of photocatalytic active $PEG_{113}$-*b*-$PAEMA_{50}$-EYHEMA (NP-AEMA-EY) or photocatalytic inactive $PEG_{113}$-*b*-$PAEMA_{50}$ (NP-PAEMA) copolymers, respectively. The photocatalytic unit was selectively polymerised at the end of the hydrophobic chain to minimise its activity until activated by the change of pH.[35,36] The RAFT end group of the polymer in this test was not removed as it has previously been shown to be non-toxic.[37] The hydrodynamic diameter of the inactive nano-assemblies was determined by dynamic light scatting (DLS). As shown in Figure 1c, the diameter of the nano-assemblies peaked at approximately 164 nm at pH 7.4, which decreased to 13 nm at pH 6.5. This sharp size change indicates the disassembly of the nano-assemblies under slightly acidic conditions, which agrees well with the pKa value (~7.2) of the block copolymer (Figure S4). Additionally, UV-Vis transmittance (Figure S5) measurement and the digital image of $PEG_{113}$-*b*-$PAEMA_{50}$ nano-assembly dispersions showed that the turbidity increased while increasing the pH value of the buffer solution. These findings further demonstrated the pH responsiveness of these nano-assemblies. Furthermore, transmission electron microspectroscopy (TEM) image has confirmed that at pH 7.4 the polymer chains are assembled into spherical gel-like nano-assemblies (Figure 1d). Additionally, TEM images also revealed the size change of pH-responsive photocatalytic nano-assemblies $PEG_{113}$-*b*-$PAEMA_{50}$-$EYHEMA_1$ from pH 7.4 to pH 6.5 (Figure S6).

The photocatalyst eosin Y is an inexpensive and biocompatible material that has been used extensively in biological applications.[38,39] Eosin Y is capable of efficiently generating singlet oxygen (Figure 2), which has been widely used for PDT.[40] In our preliminary study, with blue light irradiation molecular eosin Y (eosin Y disodium salt) can efficiently activate prodrug model compounds containing various ROS-sensitive linkers/caps, including thiol ketal, aminoacrylate, boronic acid pinacol ester, and oxalate (Table S1, Figure S8). After 2 to 4 h of light irradiation, the prodrug model compounds were activated with over 70% yield, suggesting that eosin Y photocatalyst is effective to activate a broad range of ROS-sensitive linkages.

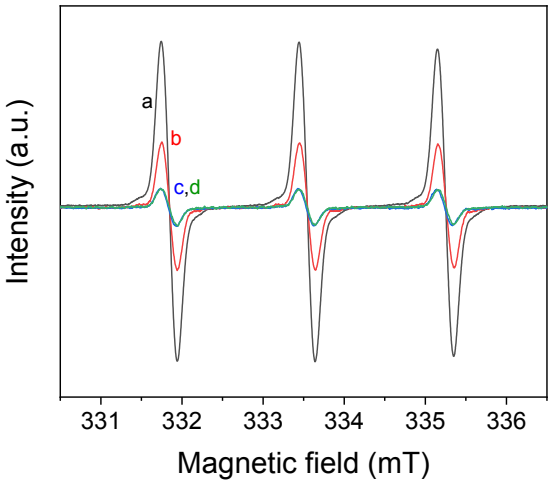


**Figure 2.** Electron paramagnetic resonance (EPR) spin trapping spectra of TEMP $^1O_2$ generated under different conditions. (a) Eosin Y disodium salt (1 mg/mL), tetramethylpiperidine (TEMP, 0.1 M), $O_2$. (b) Eosin Y disodium salt (1 mg/ml), TEMP (0.1 M), air. (c) TEMP (0.1 M), $O_2$. (d) Eosin Y disodium salt (1 mg/mL), TEMP (0.1 M), $O_2$, dark. All the samples were irradiated under blue LED for 30 min before measurement.

The promising performance of the molecular eosin Y photocatalyst in activating the prodrug model molecules has encouraged us to further examine eosin Y-based pH-responsive photocatalytic nanoparticles (NP-AEMA-EY) for the activation of prodrug model compounds. Initially, the photocatalytic activation of a prodrug model compound containing boronic acid pinacol ester was carried out using $PEG_{113}$-*b*-$PAEMA_{50}$ polymer as polymeric photocatalyst. In a typical experiment set-up, $PEG_{113}$-*b*-$PAEMAH^{+}_{50}$-$EYHEMA_1$ was

dissolved in phosphate buffer at pH 6.5 and combined with prodrug model compound in a glass vial prior to the light irradiation. The prodrug activation kinetic profiles were monitored by GCMS in triplicate. As illustrated in Figure 3, over 90% yield of activation was obtained using $PEG_{113}$-*b*-$PAEMAH^{+}_{50}$-$EYHEMA_1$ polymer as polymeric photocatalyst (2.5 mol% eosin Y moiety) after 1 h of light irradiation. When the oxygen atmosphere was replaced with air, the hydroxylation reaction progressed with a slower reaction rate compared to the reaction in the presence of oxygen. Only 16% yield was delivered after 1 h under ambient condition, suggesting the presence of oxygen is crucial for photocatalytic hydroxylation to occur efficiently. No conversion was detected for controlled reactions without photocatalyst in light and with photocatalyst in dark, respectively.

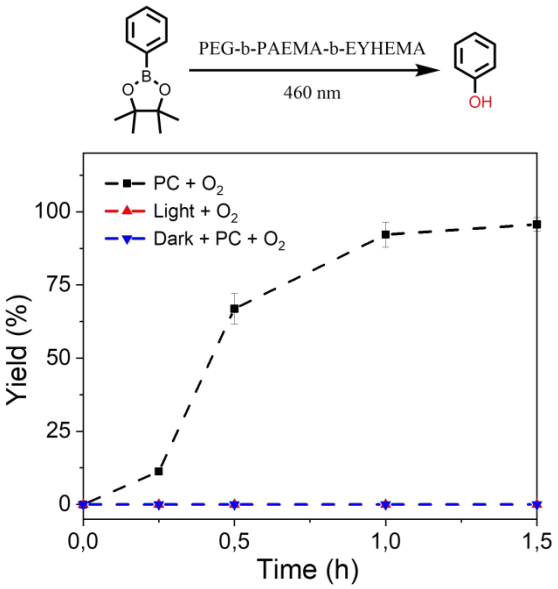


**Figure 3.** Prodrug model compound, phenylboronic acid pinacol ester, activation kinetic profile using $PEG_{113}$-*b*-$PAEMA^{+}_{50}$-EYHEMA polymeric photocatalyst (PC, 2.5 mol%) solution in phosphate buffer solution at pH 6.5 (black). Control reactions: without photocatalyst in light (green) and with photocatalyst in dark (blue).

Furthermore, we have also investigated the controlled activation of a prodrug model compound that contains a singlet oxygen sensitive aminoacrylate linker applying pH-responsive photocatalytic nanoparticle NP-AEMA-EY dispersions at pH 7.4 and $PEG_{113}$-*b*-$PAEMAH^{+}_{50}$-$EYHEMA_1$ dissolved in phosphate buffer at pH 6.5, respectively. In a typical experiment set-up, NP-AEMA-EY dispersion, or $PEG_{113}$-*b*-$PAEMAH^{+}_{50}$-$EYHEMA_1$ solution and prodrug were combined in a glass vial prior to the irradiation of blue LED light, respectively. The prodrug activation kinetic profiles were monitored by GCMS in triplicate. As we can see from Figure 4, 68% of the prodrug model compound was activated by solvated $PEG_{113}$-*b*-$PAEMAH^{+}_{50}$-$EYHEMA_1$ polymeric photocatalyst at pH 6.5 after 1.5 hours of light irradiation, whereas only 2.7% yield of activation was obtained by using NP-AEMA-EY at pH 7.4. This result strongly suggests that the photocatalyst eosin Y moieties were more accessible when the polymer chains were fully solvated at mild acidic conditions, therefore, leading to a targeted activation of prodrug model compound in the mildly acidic tumour microenvironment.

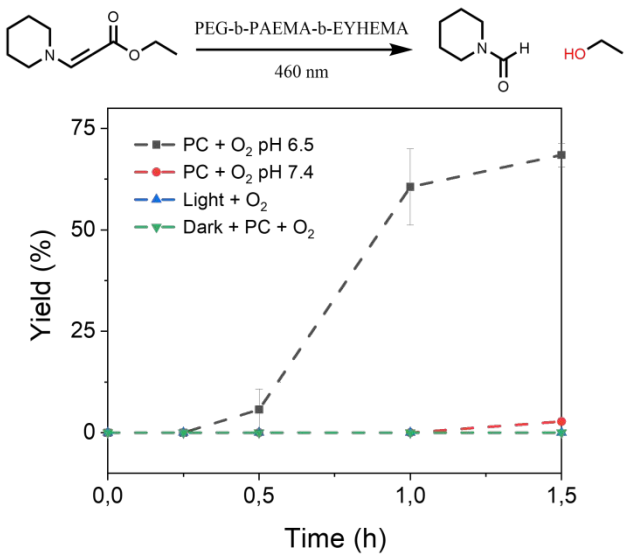


**Figure 4.** The controlled activation kinetic profile of prodrug model compound, ethyl (E)-3-(piperidin-1-yl)acrylate, using $PEG_{113}$-*b*-$PAEMA_{50}$-EYHEMA polymeric photocatalyst (PC, 2.5 mol%) solution in phosphate buffer solution at pH 6.5 (black) and NP-AEMA-EY in PBS buffer at pH 7.4 (red). Control reactions: without photocatalyst in light (green) and with photocatalyst in dark (blue).

The excellent performance of the polymeric photocatalyst in activating ROS-sensitive caping groups in a controlled manner has boosted our interest in investigating the activation of an anticancer drug molecule. 5-fluorouracial (5FU) is an FDA-approved chemotherapy drug that has been widely prescribed alone or in combination with other chemotherapeutics for various of solid tumours treatment (e.g. breast cancer, pancreatic cancer, colorectal cancer, stomach cancer, cervical cancer, and skin cancer). Over the past decades, mechanisms of the action of 5FU in the human body have been intensively studied and clearly demonstrated.[41–43] Briefly, 5FU molecules can inhibit the activity of the nucleotide synthesis enzyme thymidylate synthase (TS), which is crucial for catalyzing the reductive methylation of deoxyuridine monophosphate to deoxythymidine monophosphate. By blocking the function of TS, DNA replication and repair are interrupted.[41,43] Despite the excellent anticancer activity, major side effects of 5FU, including central neurotoxicity, gastrointestinal toxicity, and myelosuppression, as well as being metabolically unstable, still significantly limit its clinical use.[44] Therefore, prodrug strategies have been actively investigated to overcome these limitations, where several 5FU-prodrugs among many analogues have been successfully applied in clinic use.[45]

Here, 5FU was selected as an example of anticancer drug and we are interested in the creation of a ROS-sensitive 5FU-prodrug that can be selectively activated by the pH-responsive photocatalyst at the tumour site. As we have demonstrated the remarkable performance

of the pH-responsive photocatalyst in activating the boronic acid pinacol ester group, an arylboronate-based prodrug of 5FU (5-fluoro-1-(4-(4,4,5,5-tetramethyl-1,3,2-dioxaborolan-2-yl)benzyl)pyrimidine-2,4(1H,3H)-dione) has been synthesized by introducing a ROS-sensitive *p*-boronate-benzyl group to the N1 position of the 5FU according to the literature.[46] Similar to the aforementioned prodrug model compound activation procedures, the 5FU prodrug was mixed with $PEG_{113}$-*b*-$PAEMAH^{+}_{50}$-$EYHEMA_1$ solution in phosphate buffer at pH 6.5 before being subjected to light irradiation. The conversion of 5FU prodrug was monitored by 19F-NMR, where > 99% conversion of 5FU prodrug into an intermediate was obtained after half an hour of light irradiation (Figure S8). As reported in the literature,[46] this intermediate is subsequently activated spontaneously in cell culture conditions, leading to the release of active 5FU and the death of cancerous tissue.

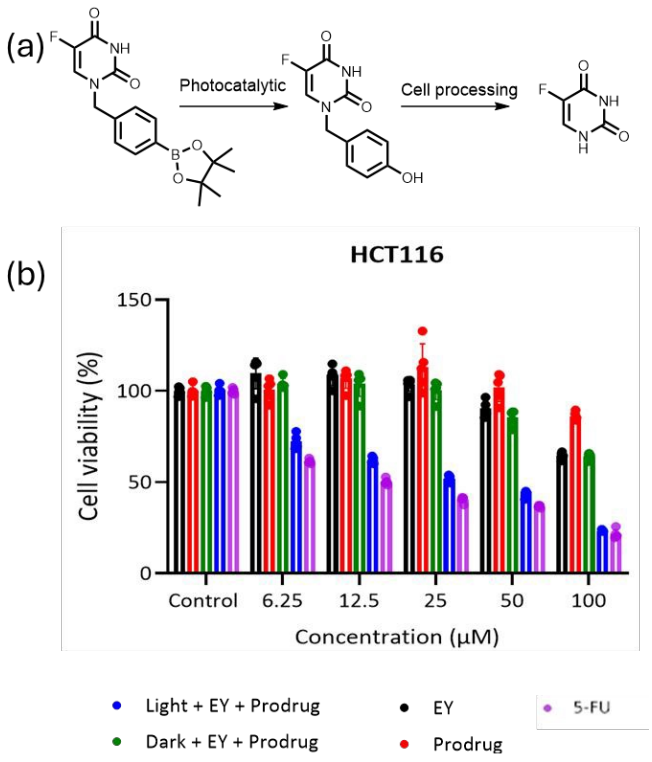


**Figure 5.** The viability of HCT116 cancer cells treated with varying concentrations of prodrug, $PEG_{113}$-*b*-$PAEMAH^{+}_{50}$-$EYHEMA_1$ (shortened as EY), the combination of prodrug and $PEG_{113}$-*b*-$PAEMA_{50}$-EYHEMA before and after blue light LED irradiation, and a control of just 5-FU. The cells were treated for 72 h with the indicated concentrations of the compounds. Data are presented as mean ± S.D, n = 5.

A cell viability study was undertaken to verify that the photocatalytically activated 5FU prodrug intermediate could subsequently be converted to 5FU and induce cell death. Here, the prodrug and photocatalyst were either irradiated or kept in dark prior to incubation with cancer cells. Additionally, control experiments of the photocatalyst and the prodrug were performed separately (Figure 5). The cell viability results showed that only the combination of prodrug, photocatalyst and light-induced cell death. This suggests that the photoactivated prodrug intermediate undergoes further activation and forms 5FU as expected, leading to cell death. As the concentration of the activated prodrug loading increased, cell viability of the group treated with combination of prodrug and photocatalytic polymer $PEG_{113}$-*b*-$PAEMAH^{+}_{50}$-$EYHEMA_1$ after blue light LED irradiation significantly decreased, indicating prominent antitumour efficacy through 5FU chemotherapy. However, the effect of the photocleaved 5FU was not as strong as the free 5FU which suggests that not all the prodrug is activated. Meanwhile, the individual components of prodrug, photocatalytic polymer $PEG_{113}$-*b*-$PAEMAH^{+}_{50}$-$EYHEMA_1$, as well as prodrug and photocatalytic polymer $PEG_{113}$-*b*-$PAEMAH^{+}_{50}$-$EYHEMA_1$ mixture in the absence of light irradiation (dark) treatments, showed negligible toxicity until high concentrations (100 uM) were applied.

In conclusion, we have designed and synthesized a novel pH-responsive polymeric photocatalyst consisting of azepane moieties as pH-responsive functional groups and a small loading of eosin Y as a photocatalyst. This polymeric photocatalytic material exhibited excellent reactivity in the activation of prodrug model compounds with different ROS-sensitive protecting groups at mild acidic conditions (pH 6.5). Moreover, the controlled activation of the prodrug model compound has been achieved, taking advantage of the ultra pH-sensitive nature (0.3 pH increment) of the polymeric photocatalyst, where a 25 times high yield of release has been obtained at pH 6.5 compared to the reaction at pH 7.4. Furthermore, this polymeric photocatalyst has efficiently activated the 5FU prodrug into an intermediate, which can be spontaneously activated into the active parent 5FU in cell cultivation. These findings demonstrate that the pH-responsive polymeric photocatalyst provides an effective approach to selectively activate prodrugs with various ROS-sensitive linkers/caps, which can potentially enhance the antitumour efficacy through PDT/chemo combination therapy.

The proof-of-principle work demonstrated here has shown the potential to use pH-responsive polymer photocatalysts to activate prodrug molecules. However, several critical factors still need to be overcome for the medical application of these systems, namely the reaction times in low-oxygen environments, the wavelength of light used, and the codelivery of the photocatalytic system and prodrug. The polymer system demonstrated here is modular, and each component can be replaced. Therefore, future work will investigate different photocatalytic species in order to increase their applicability. This is an exciting emerging area with the potential to create new therapeutic strategies.

## Conflicts of interest

"There are no conflicts to declare".

## Acknowledgement

View Article Online
DOI: 10.1039/D4PY00493K

We sincerely thank Christoph Sieber and Katrin Kirchhoff for taking TEM images. We are grateful for the funding granted by Max Planck Graduate Centre (MPGC).

## Notes and references

[1] C. T. J. Ferguson, K. A. I. Zhang, *ACS Catal.* **2021**, *11*, 9547–9560.
[2] Y. Nosaka, A. Y. Nosaka, *Chem. Rev.* **2017**, *117*, 11302–11336.
[3] Z. Zhou, J. Song, L. Nie, X. Chen, *Chem. Soc. Rev.* **2016**, *45*, 6597–6626.
[4] J. H. Correia, J. A. Rodrigues, S. Pimenta, T. Dong, Z. Yang, *Pharmaceutics* **2021**, *13*, 1332.
[5] S. Wang, G. Yu, Z. Wang, O. Jacobson, L.-S. Lin, W. Yang, H. Deng, Z. He, Y. Liu, Z.-Y. Chen, X. Chen, *Angewandte Chemie International Edition* **2019**, *58*, 14758–14763.
[6] X. Zhang, S. Wang, G. Cheng, P. Yu, J. Chang, X. Chen, *Matter* **2021**, *4*, 26–53.
[7] J. F. Lovell, T. W. B. Liu, J. Chen, G. Zheng, *Chem. Rev.* **2010**, *110*, 2839–2857.
[8] L. Cheng, C. Wang, L. Feng, K. Yang, Z. Liu, *Chem. Rev.* **2014**, *114*, 10869–10939.
[9] H. O. Alsaab, M. S. Alghamdi, A. S. Alotaibi, R. Alzhrani, F. Alwuthaynani, Y. S. Althobaiti, A. H. Almalki, S. Sau, A. K. Iyer, *Cancers* **2020**, *12*, 2793.
[10] D. Bechet, P. Couleaud, C. Frochot, M.-L. Viriot, F. Guillemin, M. Barberi-Heyob, *Trends Biotechnol* **2008**, *26*, 612–621.
[11] H. Sun, Z. Zhong, *ACS Macro Lett.* **2020**, *9*, 1292–1302.
[12] R. Wei, S. Liu, S. Zhang, L. Min, S. Zhu, *Anal Cell Pathol (Amst)* **2020**, *2020*, 6283796.
[13] R. Tong, H. H. Chiang, D. S. Kohane, *Proceedings of the National Academy of Sciences* **2013**, *110*, 19048–19053.
[14] R. Tong, H. D. Hemmati, R. Langer, D. S. Kohane, *J. Am. Chem. Soc.* **2012**, *134*, 8848–8855.
[15] S. Ruan, X. Cao, X. Cun, G. Hu, Y. Zhou, Y. Zhang, L. Lu, Q. He, H. Gao, *Biomaterials* **2015**, *60*, 100–110.
[16] Q. Zhou, *Nature Nanotechnology* **2019**, *14*, 16.
[17] Y. Dong, Y. Tu, K. Wang, C. Xu, Y. Yuan, J. Wang, *Angewandte Chemie International Edition* **2020**, *59*, 7168–7172.
[18] J. Li, Y. Li, Y. Wang, W. Ke, W. Chen, W. Wang, Z. Ge, *Nano Lett.* **2017**, *17*, 6983–6990.
[19] H.-J. Li, J.-Z. Du, J. Liu, X.-J. Du, S. Shen, Y.-H. Zhu, X. Wang, X. Ye, S. Nie, J. Wang, *ACS Nano* **2016**, *10*, 6753–6761.
[20] Z. Deng, Y. Qian, Y. Yu, G. Liu, J. Hu, G. Zhang, S. Liu, *J. Am. Chem. Soc.* **2016**, *138*, 10452–10466.
[21] S. Zhou, X. Hu, R. Xia, S. Liu, Q. Pei, G. Chen, Z. Xie, X. Jing, *Angewandte Chemie International Edition* **2020**, *59*, 23198–23205.
[22] P. Kulkarni, M. K. Haldar, P. Katti, C. Dawes, S. You, Y. Choi, S. Mallik, *Bioconjugate Chem.* **2016**, *27*, 1830–1838.
[23] P. Wang, Q. Gong, J. Hu, X. Li, X. Zhang, *J. Med. Chem.* **2021**, *64*, 298–325.
[24] M. Bio, G. Nkepang, Y. You, *Chem. Commun.* **2012**, *48*, 6517–6519.
[25] Y. Yuan, C.-J. Zhang, B. Liu, *Angewandte Chemie International Edition* **2015**, *54*, 11419–11423.
[26] Z. Cao, Y. Ma, C. Sun, Z. Lu, Z. Yao, J. Wang, D. Li, Y. Yuan, X. Yang, *Chem. Mater.* **2018**, *30*, 517–525.
[27] S. Z. F. Phua, C. Xue, W. Q. Lim, G. Yang, H. Chen, Y. Zhang, C. F. Wijaya, Z. Luo, Y. Zhao, *Chem. Mater.* **2019**, *31*, 3349–3358.
[28] Y. Kuang, K. Balakrishnan, V. Gandhi, X. Peng, *J. Am. Chem. Soc.* **2011**, *133*, 19278–19281.
[29] W. Chen, Y. Han, X. Peng, *Chemistry – A European Journal* **2014**, *20*, 7410–7418.
[30] W. Chen, K. Balakrishnan, Y. Kuang, Y. Han, M. Fu, V. Gandhi, X. Peng, *J. Med. Chem.* **2014**, *57*, 4498–4510.
[31] W. Zhang, X. Hu, Q. Shen, D. Xing, *Nat Commun* **2019**, *10*, 1704.
[32] L. Balan, J.-P. Malval, D.-J. Lougnot, **2010**.
[33] K. Zhou, Y. Wang, X. Huang, K. Luby-Phelps, B. D. Sumer, J. Gao, *Angewandte Chemie International Edition* **2011**, *50*, 6109–6114.
[34] B. A. Webb, M. Chimenti, M. P. Jacobson, D. L. Barber, *Nat Rev Cancer* **2011**, *11*, 671–677.
[35] R. Li, J. Heuer, T. Kuckhoff, K. Landfester, C. T. J. Ferguson, *Angewandte Chemie International Edition* **2023**, *62*, e202217652.
[36] J. Heuer, T. Kuckhoff, R. Li, K. Landfester, C. T. J. Ferguson, *ACS Appl. Mater. Interfaces* **2023**, *15*, 2891–2900.
[37] D. Pissuwan, C. Boyer, K. Gunasekaran, T. P. Davis, V. Bulmus, *Biomacromolecules* **2010**, *11*, 412–420.
[38] D. P. Hari, B. König, *Chem. Commun.* **2014**, *50*, 6688–6699.
[39] C. Wu, N. Corrigan, C.-H. Lim, K. Jung, J. Zhu, G. Miyake, J. Xu, C. Boyer, *Macromolecules* **2019**, *52*, 236–248.
[40] B. Fan, W. Peng, Y. Zhang, P. Liu, J. Shen, *Biomater. Sci.* **2023**, *11*, 4930–4937.
[41] D. B. Longley, D. P. Harkin, P. G. Johnston, *Nat Rev Cancer* **2003**, *3*, 330–338.
[42] G. D. Heggie, J. P. Sommadossi, D. S. Cross, W. J. Huster, R. B. Diasio, *Cancer Res* **1987**, *47*, 2203–2206.
[43] M. Scartozzi, E. Maccaroni, R. Giampieri, M. Pistelli, A. Bittoni, M. Del Prete, R. Berardi, S. Cascinu, *Pharmacogenomics* **2011**, *12*, 251–265.
[44] J. S. Macdonald, *Oncology (Williston Park)* **1999**, *13*, 33–34.
[45] J. Shelton, X. Lu, J. A. Hollenbaugh, J. H. Cho, F. Amblard, R. F. Schinazi, *Chem. Rev.* **2016**, *116*, 14379–14455.
[46] Y. Ai, O. N. Obianom, M. Kuser, Y. Li, Y. Shu, F. Xue, *ACS Med. Chem. Lett.* **2019**, *10*, 127–131.

.

View Article Online
DOI: 10.1039/D4PY00493K

The authors confirm that the data supporting the findings of this study are available within the article and its supplementary materials.